

***Emx2* and *Pax6* Control Regionalization of the Pre-neuronogenic Cortical Primordium**

Luca Muzio¹, Barbara Di Benedetto¹, Anastassia Stoykova², Edoardo Boncinelli^{1,3}, Peter Gruss² and Antonello Mallamaci¹

¹Department of Biological and Technological Research (DIBIT), Istituto Scientifico H. San Raffaele, via Olgettina 58, 20132 Milano, Italy, ²Max-Planck Institute of Biophysical Chemistry, Am Fassberg, 37018 Goettingen, Germany and ³Università Vita-Salute San Raffaele, Faculty of Psychology, via Olgettina 58, 20132 Milan, Italy

It has recently been demonstrated that the transcription factor genes *Emx2* and *Pax6*, expressed in the developing cerebral cortex along two complementary tangential gradients, are essential for the shaping of the cortical areal profile at late developmental ages, when cortical neurogenesis is almost completed. In this study we addressed the question of whether cortical regionalization is already affected in *Emx2* and *Pax6* loss of function mutants at the beginning of neurogenesis. By comparing expression patterns of selected molecular markers in these mutants at this age, we found that: (i) *Emx2* and *Pax6* are necessary for the establishment of their own specific expression profiles and are able to down-regulate each other; and (ii) absence of functional EMX2 or PAX6 proteins results in reduction of caudal–medial and rostral–lateral cortical regions, respectively, as well as in impairment of the WNT signalling center at the medial–caudal edge of the cortical field, crucial for cortical growth. These results suggest that pre-neuronogenic cortical regionalization may rely on mutual interactions between these two transcription factors and that the late areal phenotype of *Emx2*^{-/-} and *Pax6*^{-/-} mutants may possibly arise from both misconfiguration of the cortical molecular protomap and distortion of the cortical growth profile.

Introduction

In the past, mechanisms controlling arealization of the developing cerebral cortex have been the subject of a long debate (Rakic, 1988; O'Leary, 1989). Today there is a general consensus that this process largely relies on the interplay between factors intrinsic to the cortical primordium and influences coming from subcortical structures. In particular, a large body of experimental evidences suggests that cortex-autonomous molecular cues drive the early phases of arealization, independent of information delivered later by thalamic afferents. This evidence includes: (i) early patterned expression of transcription factors in the cortical primordium (Walther and Gruss, 1991; Gulisano *et al.*, 1996; Mallamaci *et al.*, 1998); (ii) establishment of *EphA*s areal expression profiles and regional commitment of late areal markers prior to the arrival of thalamic fibers (Barbe and Levitt, 1991, 1992; Arimatsu *et al.*, 1992; Ferri and Levitt, 1993; Donoghue and Rakic, 1999; Gitton *et al.*, 1999); and (iii) areal restriction of *Cadherins* gene products in the cortex of mutants lacking thalamo-cortical connections (Miyashita-Lin *et al.*, 1999; Nakagawa *et al.*, 1999). However, little is known about mechanisms controlling the development of the early cortical molecular protomap.

It has been demonstrated recently that the transcription factor genes *Emx2* and *Pax6*, expressed in the cortical pseudostratified ventricular epithelium (PVE) along two complementary tangential gradients (Walther and Gruss, 1991; Gulisano *et al.*, 1996; Mallamaci *et al.*, 1998), are essential for the proper shaping of the cortical areal profile. In the absence of *Emx2*, a dramatic reduction of cortical regions with caudal–medial identity takes place, together with an enlargement of those with

rostral–lateral identity (Bishop *et al.*, 2000; Mallamaci *et al.*, 2000). Complementary phenotype has been described in *Pax6* homozygous (*Sey/Sey*) mutants (Bishop *et al.*, 2000). Assessments of areal profiles in these mutants were made by a variety of experimental approaches, but only after the end of primary neurogenesis; mechanisms underlying the genesis of the areal phenotypes were not extensively addressed. In particular, it was not established whether the *Emx2*^{-/-} and *Pax6*^{-/-} phenotypes are simply due to a distorted tangential growth of the PVE after its areal commitment, or whether they reflect an altered regionalization of the PVE prior to this commitment. These two hypotheses are not mutually exclusive.

At the onset of the primary neurogenesis, a number of genes, including the homeobox genes *Emx2* (Simeone *et al.*, 1992; Gulisano *et al.*, 1996; Mallamaci *et al.*, 1998), *Pax6* (Walther and Gruss, 1991; Stoykova and Gruss, 1994) and *Emx1* (Simeone *et al.*, 1992; Briata *et al.*, 1996; Gulisano *et al.*, 1996), the T-box gene *Tbr2* (Bulfone *et al.*, 1999; Kimura *et al.*, 1999), the secreted factor genes *Wnt3a* (Roelink and Nusse, 1991; Grove *et al.*, 1998), *Wnt8b* (Grove *et al.*, 1998; Lee *et al.*, 2000) and *Sfrp2* (Ragsdale *et al.*, 2000), and the FGF receptor gene *Fgfr3* (Ragsdale *et al.*, 2000), are expressed in the cortical primordium in graded ways along the tangential axes. It can reasonably be assumed that specific combinations of these genes, expressed by neuroblasts in different regions of this primordium, provide us with valuable information about latent areal values characterizing these regions. Moreover, special functional significance has to be attributed to the expression profiles of the *Wnt* genes, proven to play crucial roles in controlling growth of the cortical neuroepithelium (Lee *et al.*, 2000; McLaughlin *et al.*, 2000). Therefore, in order to cast light onto mechanisms leading to the late areal phenotypes of *Emx2* and *Pax6* null mutants, we systematically studied the expression profiles of the above-mentioned markers in the cortical anlage of wild-type, *Emx2*^{-/-} and *Pax6*^{-/-} mouse embryonic brains at the beginning of neurogenesis. We found that both EMX2 and PAX6 proteins are necessary to allow the graded expression of the corresponding genes and to down-regulate the activity of each other. In the absence of functional alleles of *Emx2* or *Pax6*, size reductions of regions with caudal–medial and rostral–lateral molecular identities, respectively, take place, accompanied by complementary changes in the cortical expression patterns of WNT signalling genes. This suggests that the proper setting up of the early cortical molecular protomap largely relies on the mutual interaction between these two transcription factors, and that the late areal phenotype of *Emx2*^{-/-} and *Pax6*^{-/-} embryos possibly reflects a misconfiguration of this protomap. Furthermore, the results imply that the late *Emx2*^{-/-} and *Pax6*^{-/-} areal phenotypes might be additionally worsened by a distorted cortical growth, as a result of an impairment of the WNT signalling center in the mutant cortex.

Materials and Methods

Animal Husbandry, Recovery of Embryos and Tissue Sampling

Pax6 mutant embryos were obtained by intercrossing viable heterozygous *Small eye* mutants, *Sey* allele (Roberts, 1967). *Sey/Sey* (hereafter called *Pax6*^{-/-}) embryos were recognized by the absence of eyes, *Sey*^{+/+} embryos by ocular abnormalities. The point mutation in the *Pax6* gene results in the generation of truncated nonfunctional protein (Hill *et al.*, 1991), whereas the transcription is not affected, thus allowing study of the activity of the gene in the affected brain regions. *Emx2* mutant embryos were obtained by intercrossing viable *Emx2*^{-/-} mutants. Embryos were genotyped by Southern analysis as described previously (Pellegrini *et al.*, 1996).

Pregnant females were anesthetized by CO₂ and killed by cervical dislocation, in compliance with European laws [European Communities Council Directive of November 24, 1986 (86/609/EEC)] and according to guidelines of H. San Raffaele Institutional Animal Care and Use Committee. Embryos were fixed in 4% paraformaldehyde-phosphate-buffered saline (PBS) overnight at +4°C and then washed, dehydrated and embedded in wax according to standard protocols. Embryonic brains were subsequently cut at 10 μm and sections were mounted on Fischer SuperFrost Plus slides. Samples were subsequently dewaxed by xylene, rehydrated in descending ethanol series and processed for *in situ* hybridization or immunohistochemistry. Unless otherwise stated, for each experiment at least three embryos per mutant genotype were analysed, together with three littermate wild-type controls.

In situ Hybridization

Sense and anti-sense riboprobes were prepared by appropriately linearizing and transcribing *Emx2*, *Pax6*, *Mash1*, *Tbr2*, *Wnt8b*, *Wnt3a*, *Sfrp2* and *Fgfr3* cDNA clones. The *Emx2* cDNA clone contained a 0.8 kbp fragment, encompassing 0.3 kbp of 5'-UTR plus 0.5 kbp of cds. The *Pax6* cDNA clone contained a 3'-UTR 965 bp fragment, amplified by PCR and corresponding to nt 1485–2450 of Genbank file NM-013627. The *Mash1* cDNA clone contained a 796 bp fragment encompassing 582 bp of 5'-UTR plus 214 bp of cds, amplified by PCR on the basis of sequence data assembled from Genbank files NM008553 and MMU68534. The *Tbr2* cDNA clone contained a 2.7 kbp fragment, encompassing 5'-UTR, cds and 3'-UTR, and was obtained from Dr Alessandro Bulfone (Milan). The *Wnt8b* cDNA clone contained a 1370 bp fragment, encompassing the last 488 bp of cds plus the first 882 bp of the 3'-UTR, amplified by PCR on the basis of sequence data from Genbank files NM-011172, AW488375 and AA874401. The *Wnt3a* cDNA clone contained a 1421 bp fragment of 3'-UTR, amplified by PCR and corresponding to nt 1213–2634 of Genbank file NM-009522.1. The *Sfrp2* cDNA clone contained a 798 bp fragment of 3'-UTR, amplified by PCR and corresponding to nt 1127–1925 of Genbank file MMU88567. The *Fgfr3* cDNA clone contained a 897 bp fragment of 3'-UTR, amplified by PCR and corresponding to nt 829–1726 of Genbank file L42132. Non-radioactive *in situ* hybridization was performed as described in Bovolenta *et al.* (Bovolenta *et al.*, 1997).

Immunohistochemistry

Antigens were unmasked by boiling samples in 10 mM sodium citrate, pH 6.0, for 5 min and allowing them to cool down slowly, prior to applying conventional immunohistochemical protocols (Mallamaci *et al.*, 1998). The following primary antibodies were used: α-EMX1, rabbit polyclonal (Briata *et al.*, 1996), 1:400; α-neuron-specific class III β-tubulin, mouse monoclonal (clone Tuj1; BabCo, Richmond, CA), 1:100.

Photography and Editing

Micrographs of the immunohistochemical preparations were taken using an SV Micro CV3000 digital microscope camera (Taunton, MA). Electronic files were processed on a MacIntoshG3 computer using Adobe Photoshop 5.0 software (San Jose, CA).

EMX1, Tbr2 and Wnt8b Morphometry

Wax embedded brains were cut at 10 μm in the coronal plane. Every seventh section was processed for *Wnt8b in situ* hybridization and single sections immediately after in the series were processed for α-EMX1 immunohistochemistry, *Mash1 in situ* hybridization, *Tbr2 in situ* hybridization and Tuj1 immunohistochemistry. After taking photographs

of the sections, the *Mash1* expression profiles were electronically copied onto EMX1 images, the Tuj1 and the EMX1 profiles onto *Tbr2* images, and the EMX1 profiles onto *Wnt8b* pictures. Medial-lateral extensions of the cortical PVE subdomains expressing EMX1, *Tbr2* and *Wnt8b* were measured on each section by two independent investigators blind to genotype. In the case of EMX1 and *Wnt8b*, the lateral boundaries of their expression domains were placed on the computer screen using Adobe Photoshop 5.0 (San Jose, CA) software and always referring to given sets of chromatic parameters. In the case of *Tbr2*, in order clearly to distinguish lateral PVE, where *Tbr2* positive cells are tightly clustered, from medial PVE, where only a few *Tbr2* positive cells can be found, PVE was partitioned into equally spaced radial sectors, each extending for 50 μm of the pallial ventricular boundary. *Tbr2* positive cells were counted in each sector and those bearing five or more cells (corresponding to ≥1 cell/10 μm) were classified as 'high density', those bearing fewer cells as 'low density'. This analysis was performed in parallel on five *Emx2*^{-/-} and three wild-type littermates, as well as on five *Pax6*^{-/-} and three wild-type littermates, at E11. Data from animals of each genotype, relative to rostral, intermediate and caudal thirds of the cortical primordium (EMX1 and *Tbr2*) or to the whole primordium (*Wnt8b*), were averaged and ratios between extensions of lateral and medial subfields were calculated; statistical significance of differences was evaluated by Student's *t*-test and results synthesized in Figures 2H,P and 4E.

Wnt3a Morphometry

Fixed and wax-embedded brains were cut at 10 μm in the coronal plane. Every fourth section was processed for *Wnt3a in situ* hybridization and photographed as described above. The rostro-caudal extension of the cortico-diencephalic boundary and *Wnt3a* expression domain were determined by inspecting all micrographs; the relative rostro-caudal extension of the *Wnt3a* expression domain along this boundary was subsequently calculated. This analysis was performed in parallel on five *Emx2*^{-/-} and three wild-type littermates, as well as on five *Pax6*^{-/-} and three wild-type littermates, at E11. Data from animals of each genotype were averaged; statistical significance of differences was evaluated by Student's *t*-test and results finally synthesized in Figure 4P.

Results

Interactions between Emx2 and Pax6

In order to examine whether an interplay between *Emx2* and *Pax6* might be involved in the control of early cortical regionalization, we compared expression patterns of these two genes in the cortical primordium of wild-type, *Emx2* null and *Pax6* null mutant mice, at the beginning of neocortical neuronogenesis. Using normal embryos, we confirmed previous reports (Walther and Gruss, 1991; Gulisano *et al.*, 1996; Mallamaci *et al.*, 1998) on the existence of two complementary medial-lateral expression gradients, an *Emx2* gradient increasing medially and a *Pax6* gradient showing increased expression levels laterally (Fig. 1B,E). In both *Emx2* and *Pax6* null mutants, dramatic changes of *Emx2* and *Pax6* expression profiles were detectable. *Emx2* expression was down-regulated in the medial cortex of *Emx2* mutants (Fig. 1A), thus flattening the normal medial-high to lateral-low expression gradient. *Emx2* expression spread more laterally in *Pax6* null mutants, almost abolishing the normal expression gradient (Fig. 1C). *Pax6* expression was enhanced in the medial cortical anlage of *Pax6* mutants, thus flattening the normal medial-low to lateral-high expression gradient (Fig. 1F). *Pax6* expression was also up-regulated in the entire cortical field of *Emx2* null mutants, which conversely still displayed a properly oriented expression gradient (Fig. 1D). Thus, the generation of the opposite *Emx2* and *Pax6* expression gradients appears to depend on the availability of functional EMX2 and PAX6 proteins, respectively, and the average expression levels of *Emx2* and *Pax6* arise in the absence of functional PAX6 and EMX2 proteins, respectively.

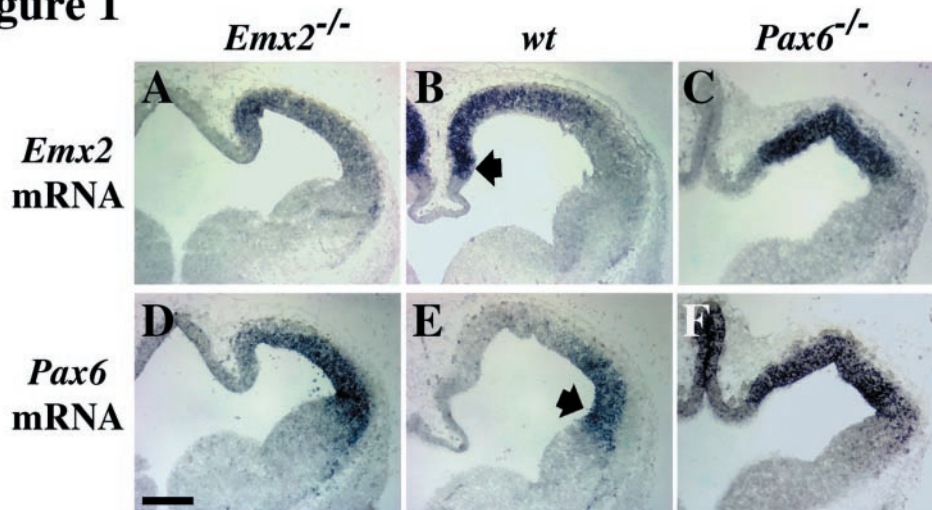
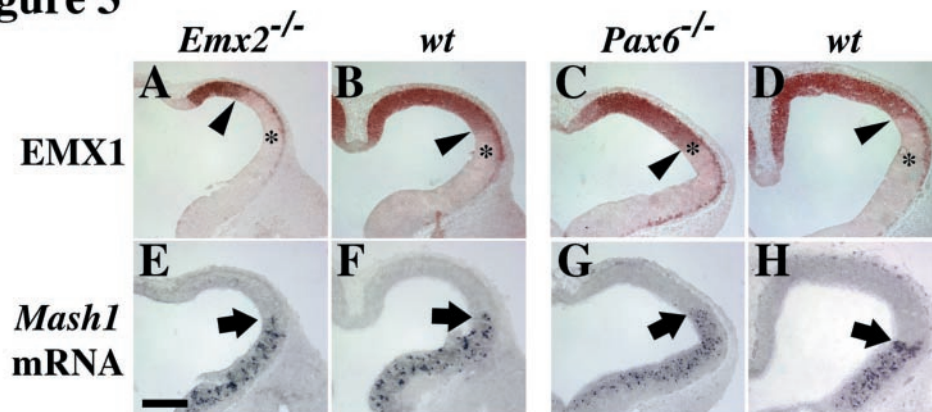
Figure 1**Figure 3**

Figure 1. Distribution of *Emx2* (A–C) and *Pax6* (D–F) transcripts on mid-frontal sections of *Emx2*^{−/−} (A, D), wild-type (B, E) and *Pax6*^{−/−} (C, F) E11 murine telencephalons. In wild-type embryos, *Emx2* and *Pax6* are gradedly expressed in the alar telencephalic wall along two medial–lateral complementary gradients. The former has its maximum near the boundary between cortex and cortical hem (arrow in B), the latter has its maximum near the pallial–subpallial border within the LGE (arrow in E). In *Emx2*^{−/−} embryos, *Emx2* is medially down-regulated and its gradient flattened (A), *Pax6* is up-regulated and its expression spreads medially (D). In *Pax6*^{−/−} embryos, *Emx2* is laterally up-regulated and its gradient flattened (C), *Pax6* is up-regulated in the dorso-medial cortex and its gradient flattened (F). Scale bar: 200 μm.

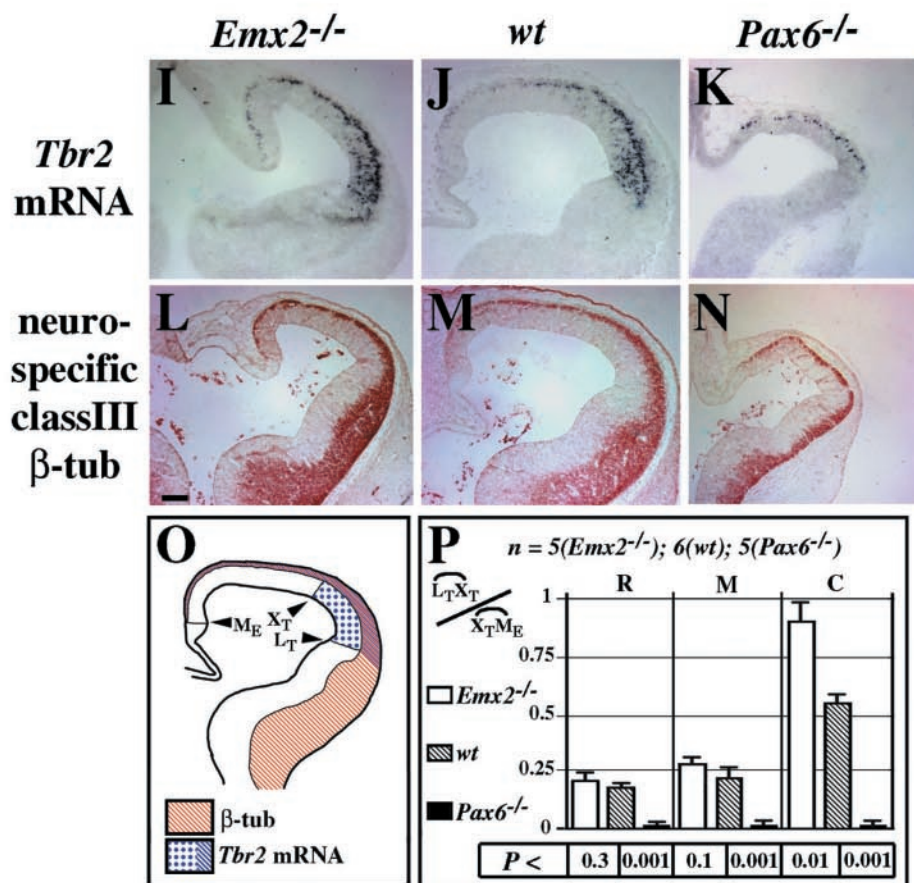
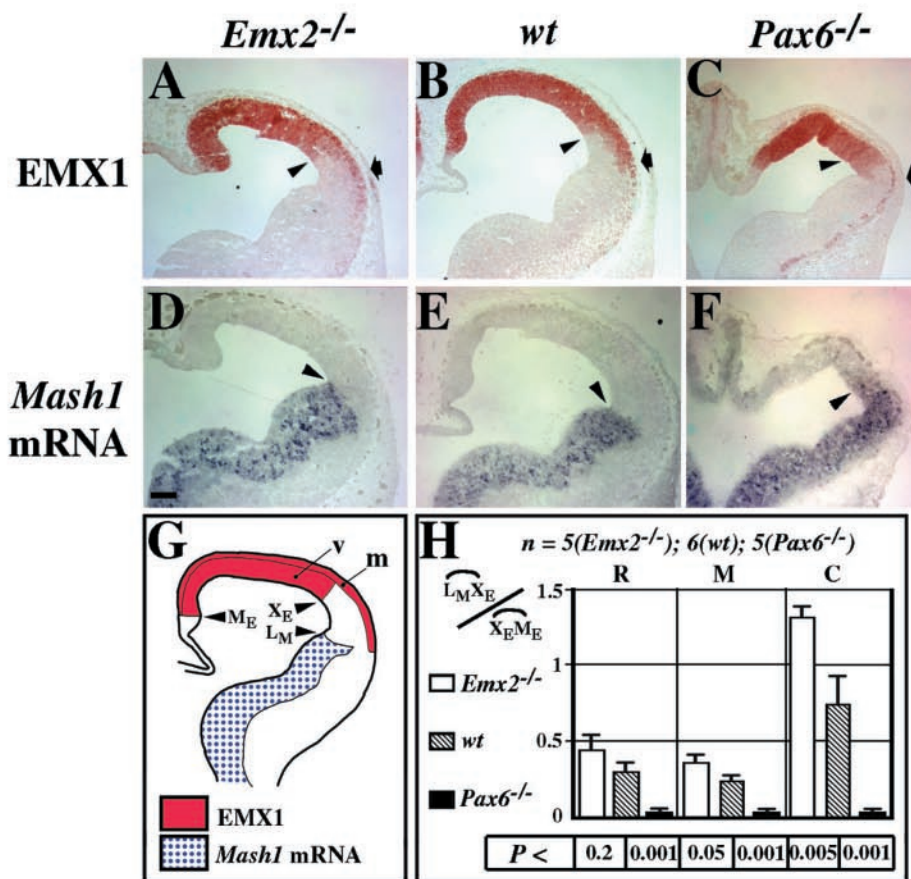
Figure 3. Distribution of the EMX1 homeoprotein (A–D) and of the *Mash1* mRNA (E–H) on adjacent frontal sections from telencephalons of *Emx2*^{−/−} (A, E), wild-type (B, D, F, H) and *Pax6*^{−/−} (C, G) E10 mouse embryos; sections (A, B, E, F) were taken from more caudal axial levels as compared with sections (C, D, G, H). The distribution of *Emx1* and *Mash1* products is very similar to that found at E11 (Fig. 2), with EMX1 confined to the presumptive archi-neocortical field and *Mash1* mRNA expressed in the basal forebrain. Arrowheads point to ventral boundary of the EMX1 ventricular domain (A–D); arrows point to dorsal boundary of the *Mash1* expression domain (E–H); asterisks indicate presumptive dorsal boundary of *Mash1* mRNA on anti-EMX1 probed sections (A–D), as estimated by graphic interpolation. Remarkably, medial–lateral extension of the lateral *Mash1* mRNA[−]/EMX1[−] domain (encompassed between arrowhead and asterisk) is enlarged in *Emx2*^{−/−} mutants and reduced to almost zero in *Pax6*^{−/−} mutants; conversely, the EMX1⁺ domain is reduced in both mutants, much more, however, in *Emx2*^{−/−} than in *Pax6*^{−/−} mutants. Scale bar: 200 μm.

Emx1 and Tbr2 Expression Patterns in *Emx2* and *Pax6* Null Brains

In order to obtain information about areal values characterizing different regions of the early cortical primordium in the absence of *Emx2* or *Pax6*, we selected two transcription factor genes whose expression normally displays specific regional restrictions in this primordium, the homeobox gene *Emx1* (Simeone *et al.*, 1992; Briata *et al.*, 1996; Gulisano *et al.*, 1996) and the T-box gene *Tbr2* (Bulfone *et al.*, 1999; Kimura *et al.*, 1999) and

compared their expression profiles in E11 wild-type, *Emx2*^{−/−} and *Pax6*^{−/−} brains.

EMX1 immunoreactivity could be detected in two cortical domains, in the primordial plexiform layer (PPL) as well as in the PVE (Fig. 2B, G). These domains could be easily distinguished by comparing EMX1 immunoreactivity (Fig. 2B) with immunoreactivity against class-III-neuron-specific β-tubulin, specifically detectable in post-mitotic neurons of the PPL (Fig. 2M). *Emx1* products were abundant in the medial PVE, but fell below



detectability threshold in the lateral part (Fig. 2B,G); thus, at E11, the cortical anlage could be divided into two subfields – a medial subfield, where the PVE is strongly immunoreactive for EMX1 (EMX1⁺ subfield) and a lateral one, where the PVE is EMX1 negative (EMX1⁻ subfield). To estimate medial–lateral extensions of these subfields, it was necessary to define borders of the entire cortical field; for this purpose, it seemed reasonable to choose the medial boundary of EMX1 domain as medial border of the cortical field (M_E, Fig. 2B,G) and the dorsal boundary of the *Mash1* expression domain as the lateral border (L_M, Fig. 2E,G). By superimposing EMX1 and *Mash1* expression profiles from adjacent sections, it was possible to evaluate transverse extensions of EMX1⁻ and EMX1⁺ cortical subfields at different rostro-caudal locations. Data relative to rostral, intermediate and caudal thirds of the cortical primordium were averaged and ratios between extensions of lateral EMX1⁻ and medial EMX1⁺ subfields were calculated for these three different axial levels. This analysis was performed in parallel on wild-type (Fig. 2B,E), *Emx2*^{-/-} (Fig. 2A,D) and *Pax6*^{-/-} (Fig. 2C,F) embryos and results were synthesized in Figure 2H. We found that the relative extension of the lateral cortical subfield was significantly increased in *Emx2* null mutants and this phenomenon was much more pronounced in caudal as compared with rostral sections. On the other hand, the lateral subfield was dramatically reduced or even disappeared in *Pax6* null brains, at all rostro-caudal levels.

Emx1 and *Mash1* expression profiles were also studied in telencephalons of E10 embryos, where cortical neuronogenesis is just beginning, and results similar to E11 were obtained. In *Emx2*^{-/-} mutants, the cortical EMX1⁺ domain was reduced in its absolute and relative medial–lateral extension, more dramatically in the caudal half of the telencephalic vesicle (Fig. 3A,B). An absolute shrinking of the EMX1⁺ domain could also be noted in *Pax6*^{-/-} mutants, where, however, relative extension of the EMX1⁺ domain in the *Mash1*⁻ cortical field did not decrease (Fig. 3C,D). Remarkably, the EMX1⁻/*Mash1*⁻ presumptive lateral cortical field was significantly enlarged in the caudal telencephalon of *Emx2*^{-/-} mutants (Fig. 3A,B,E,F) and almost suppressed in the rostral telencephalon of *Pax6*^{-/-} mutants (Fig. 3C,D,G,H).

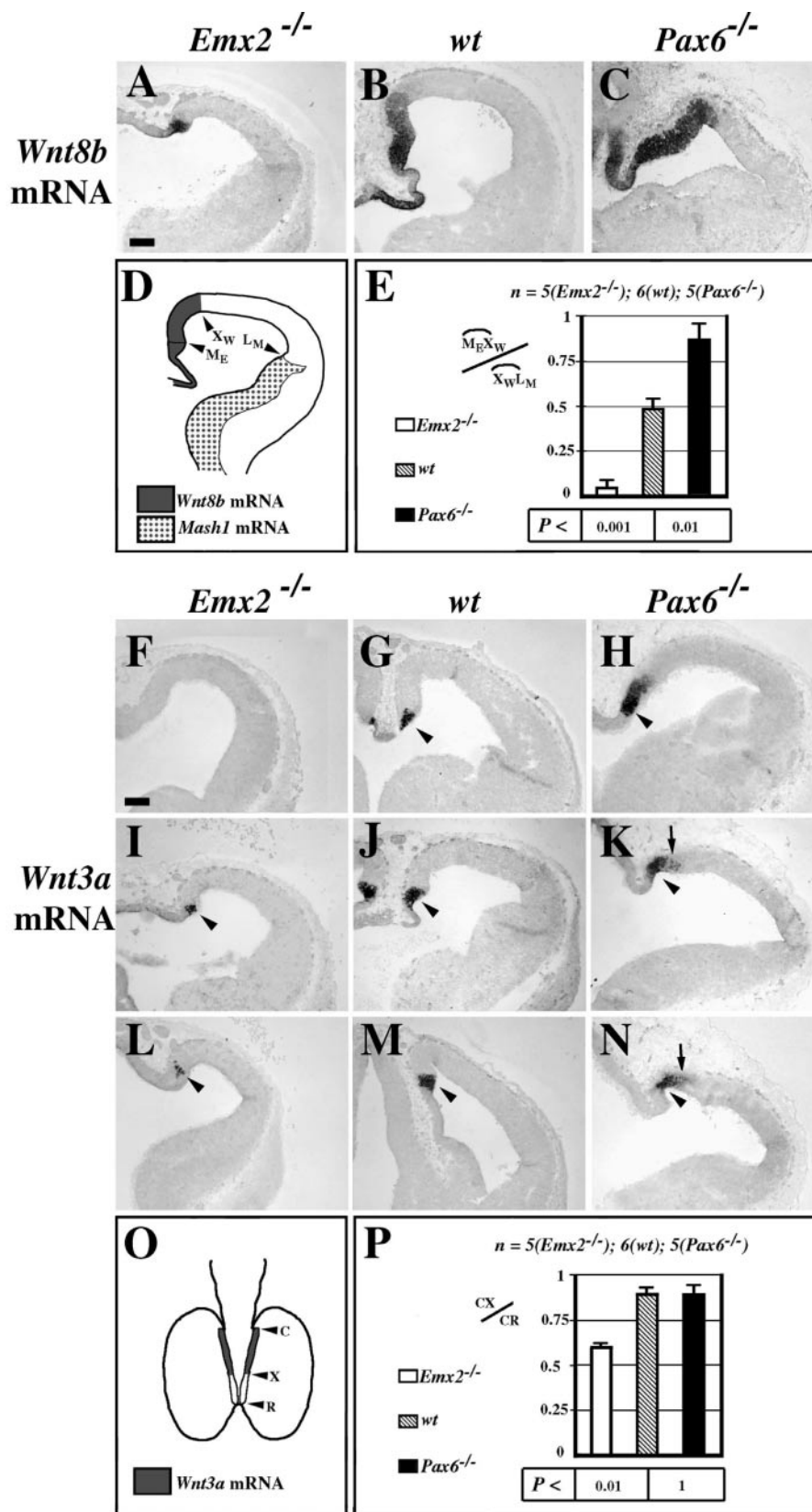
At E11, *Tbr2* products were detectable in a large subset of neurons in the PPL, as well as in a relatively small number of cells in the PVE (Figs 2J, 6B). *Tbr2* expression in the PVE was not

uniform along the medial–lateral axis; cells expressing *Tbr2* were tightly clustered in the lateral part of the PVE and were much rarer in the medial portion (Fig. 2J,O). Thus, two cortical subfields could be distinguished: a lateral one (*Tbr2*⁺ subfield), where >1 *Tbr2*⁺ cell/10 μm of free ventricular profile could be counted and a medial one (*Tbr2*⁻ subfield), where the linear density of *Tbr2*⁺ cells in the PVE abruptly fell far below this threshold. Assuming again the medial boundary of the *Emx1* as the medial edge of the cortical field, the transverse extensions of the these two cortical subfields could be measured. Data relative to rostral, intermediate and caudal thirds of the cortical primordium were averaged and ratios between extensions of the lateral and medial subfields were calculated for these three different axial levels. This analysis was performed in parallel on wild-type (Fig. 2J,M), *Emx2*^{-/-} (Fig. 2I,L) and *Pax6*^{-/-} (Fig. 2K,N) embryos and the results are summarized in Figure 2P. We found that the relative extension of the lateral *Tbr2*⁺ subfield was significantly increased in the caudal third of *Emx2* null mutants. Conversely, the lateral *Tbr2*⁺ subfield was dramatically reduced in *Pax6* null embryos at all rostro-caudal levels. If we assume that activation of *Tbr2* in cells in the ventricular zone at a spatial frequency >1 cell/10 μm of free ventricular profile is a regional property of the lateral pallial field, the almost complete absence of such cells in *Pax6* mutants can be interpreted as an index of shifting of the lateral pallial field toward a different, more medial, identity. The distribution of *Tbr2* transcripts along the rostro-caudal axis was also examined on horizontal sections, taken at an intermediate dorso-ventral level. In wild-type embryos, numerous *Tbr2* positive cells were seen in the PPL along the entire rostro-caudal axis (Fig. 6B, delimited by arrowheads), except for the caudal–medial-most part of the cortical primordium (Fig. 6B, asterisk). In both *Emx2*^{-/-} and *Pax6*^{-/-} mutant brains, the medial-most sector of the caudal cortical primordium was, conversely, populated by *Tbr2*⁺ cells (Fig. 6A,C).

WNT Signalling Genes in *Emx2* and *Pax6* Null Mutants

Several genes involved in WNT signalling are expressed in the early cortical primordium in a highly patterned way. *Wnt* expression domains, including those of *Wnt3a* and *Wnt8b*, are hemi-nested around the caudal–medial edge of the cortical

Figure 2. (A–H) Telencephalic expression domains of the homeoprotein EMX1 (A–C) and the proneural gene *Mash1* mRNA (D–F) on adjacent mid-frontal sections of *Emx2*^{-/-} (A, D), wild-type (B, E) and *Pax6*^{-/-} (C, F) E11 murine embryos. In all three genotypes, EMX1 is detectable in the alar telencephalic wall. It is in a few rows of presumptive post-mitotic cells located underneath the pial surface, along its entire medial–lateral extension (A–C, arrows). In addition, it is detectable in the underlying pseudostratified ventricular epithelium, where its expression level is medially high and laterally (beyond arrowheads in A–C) very low or absent. *Mash1* expression is confined to the basal forebrain in *Emx2*^{-/-} and wild-type embryos, falling the dorsal edge of its domain at the pallial–subpallial border, just ventral to the cortico-striatal notch (D, E, arrowheads); conversely, its expression spreads into the alar telencephalon of *Pax6*^{-/-} mutants (F, arrowhead). In (G), idealized representations of EMX1 and *Mash1* expression domains are superimposed onto a midfrontal cortical silhouette; marginal (m) and ventricular (v) EMX1 subdomains are distinguished. Arrowheads point to the dorsal edge of the *Mash1* domain, L_M, as well as to the lateral and the medial edges of the EMX1 ventricular domain, X_E and M_E, respectively. The ratio between lateral–medial extensions of the cortical ventricular EMX1⁻/*Mash1*⁻ domain, L_MX_E, and the EMX1⁺/*Mash1*⁻ domain, X_EM_E, was calculated for rostral, R, intermediate, M, and caudal, C, thirds of telencephalic vesicles of *Emx2*^{-/-}, wild-type and *Pax6*^{-/-} embryos. Results are synthesized in the histogram in (H) and *P* values relative to observed differences are listed in the box below. This analysis showed that *Emx2* null embryos display relative enlargement of lateral as compared to medial cortex, more pronounced caudally than rostrally, and that, conversely, in *Pax6* null embryos the lateral cortical domain is almost completely suppressed. Scale bar: 100 μm. (I–P). Telencephalic expression domains of the T-box transcription factor gene *Tbr2* (I–K) and the class III neuro-specific β-tubulin (L–N), on adjacent mid-frontal sections of *Emx2*^{-/-} (I, L), wild-type (J, M) and *Pax6*^{-/-} (K, N) E11 murine embryos. In all three genotypes, TuJ1 immunoreactivity can be found in the cortical primordium plexiform layer, as well as in adventricular layers of the basal telencephalon (L–N). *Tbr2* mRNA is detectable in the primordium plexiform layer of the alar telencephalon; here, *Tbr2* transcripts regionally colocalize with TuJ1 immunoreactivity. In both *Emx2* mutants and normal embryos, *Tbr2* mRNA is also detectable in cortical ventricular cells, very rare in the medial pallium and tightly clustered toward the lateral edge of the cortical morphogenetic field. It is possible to distinguish a lateral ventricular domain, where >10 *Tbr2*⁺ cells/100 μm of medial–lateral ventricular profile can be detected, and a medial ventricular domain, where far less than 10 *Tbr2*⁺ cells/100 μm can be found (I, J). *Tbr2*⁺ cells are, conversely, very rare and almost absent in the cortical PVE of *Pax6* mutants, throughout its medial–lateral extension (K). In (O), idealized representations of *Tbr2* mRNA expression domains and TuJ1 immunoreactivity are superimposed onto a midfrontal cortical silhouette. Two arrowheads point to lateral and medial boundaries of the lateral cortical ventricular domain, where *Tbr2* mRNA⁺ cells are tightly clustered, L_T and X_T, the former considered as lateral edge of the cortical field. An arrowhead points to the dorsal boundary of the EMX1 cortical domain, M_E, considered as medial edge of the cortical field. The ratio between average values of L_TX_T and X_TM_E, was calculated for rostral, R, intermediate, M, and caudal, C, thirds of telencephalic vesicles of *Emx2*^{-/-}, wild-type and *Pax6*^{-/-} embryos. Results are synthesized in the histogram in (P) and *P* values relative to observed differences are listed in the box below. This analysis showed that *Emx2* null embryos display a relative enlargement of caudal–lateral cortex as compared with caudal–medial cortex and that, in *Pax6* null embryos, the lateral cortical domain is almost completely suppressed throughout the rostro-caudal axis. Scale bar: 100 μm.



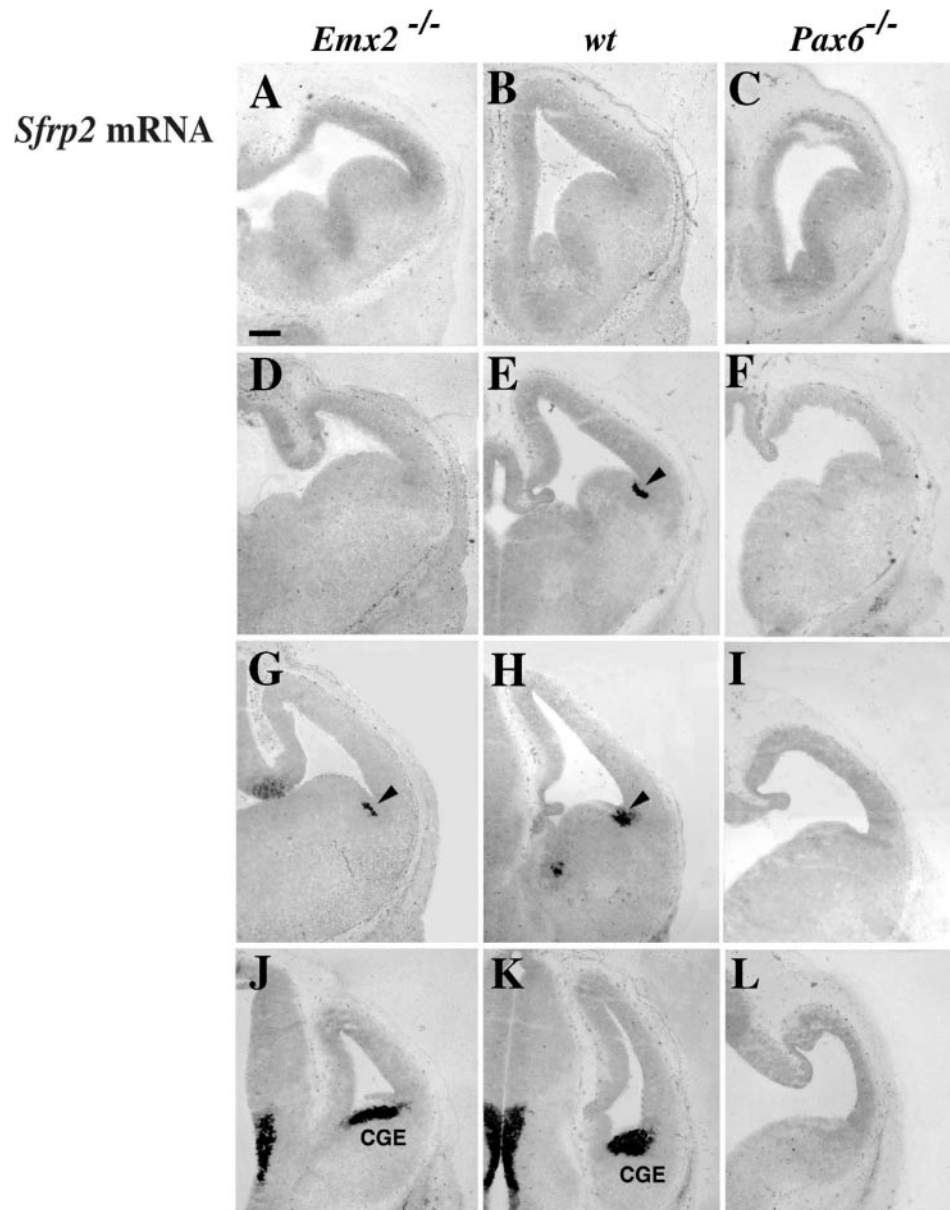


Figure 5. Distribution of *Sfrp2* mRNA on frontal sections of *Emx2*^{-/-} (A, D, G, J), wild-type (B, E, H, K) and *Pax6*^{-/-} (C, F, I, L) E12.5 murine telencephalons, taken at rostral (A–C), rostral-intermediate (D–F), caudal-intermediate (G–I) and caudal (J–L) axial levels. *Sfrp2* is expressed in the caudal ganglionic eminence (K, CGE); moreover, its mRNA can normally be detected in the lateral-most lateral ganglionic eminence, at intermediate (E, H, arrowheads) but not at rostral (B) axial levels. In *Emx2*^{-/-} mutants, *Sfrp2* mRNA is confined to the CGE (J) and to the caudal-most lateral LGE (G); it is absent in the anterior-intermediate lateral ganglionic eminence (A, B). No *Sfrp2* expression can be finally detected in the telencephalon of *Pax6*^{-/-} mutants (C, F, I, L). Scale bar: 200 μ m.

Figure 4. (A–E) Distribution of *Wnt8b* mRNA on midfrontal sections of *Emx2*^{-/-} (A), wild-type (B) and *Pax6*^{-/-} (C) E11 murine telencephalons. *Wnt8b* is expressed in the medial alar telencephalic wall, in a medially high to laterally low graded way. Relative medio-lateral extension of the *Wnt8b* cortical domain is lower in *Emx2*^{-/-} as compared with normal brains and higher in *Pax6*^{-/-} brains. In (D), an idealized representation of *Wnt8b* expression domain is superimposed on a midfrontal cortical silhouette, together with representations of EMX1 and *Mash1* domains (see Fig. 2G); arrowheads point to the medial edge of EMX1 domain, M_E, the lateral edge of *Wnt8b* domain, X_{WL}, and the dorsal boundary of *Mash1* domain, L_M. Ratios between average medial-lateral extensions of the cortical *Wnt8b*⁺ and *Wnt8b*⁻ domains, M_EX_{WL} and X_{WL}L_M, respectively, were calculated for brains of *Emx2*^{-/-}, wild-type and *Pax6*^{-/-} embryos. Results are synthesized in the histogram in (E) and *P* values relative to observed differences are listed in the box below. This analysis showed that *Emx2* null embryos display a severe reduction of the medial cortex and that, conversely, in *Pax6* null embryos this medial cortical domain is significantly enlarged. Scale bar: 100 μ m. (F–J). Distribution of *Wnt3a* mRNA on frontal sections of *Emx2*^{-/-} (F, I, L), wild-type (G, J, M) and *Pax6*^{-/-} (H, K, N) E11 murine telencephalons, taken at rostral (F, G, H), intermediate (I, J, K) and caudal (L, M, N) axial levels. In normal brains, *Wnt3a* is confined to the cortical hem (G, J, M, arrowheads); similar distribution can be detected in *Emx2*^{-/-} and *Pax6*^{-/-} mutants (F, I, L and H, K, N, arrowheads, respectively), with some differences. The *Wnt3a* domain is dramatically shrunken in *Emx2*^{-/-} mice, along both the rostro-caudal (F) and medial-lateral axes (I, L). *Wnt3a* mRNA is not properly restricted to the hem of *Pax6*^{-/-} mice, where numerous positive cells can be ectopically found in the adjacent cortex (K, N, arrows). In (D) an idealized dorsal view of an E11 telencephalon is represented, with the expression domain of *Wnt3a* in the caudal part (C-X) of the cortical hem (C-R). Relative rostro-caudal extensions of the *Wnt3a* expression domain in the hem, CX/CR, were calculated for *Emx2*^{-/-}, wild-type and *Pax6*^{-/-} genotypes. Results are synthesized in the histogram in (P) and *P* values relative to observed differences are listed in the box below. No differences are detectable between wild-type and *Pax6*^{-/-} mutants; *Wnt3a* domain is, conversely, shortened by about one-third in *Emx2*^{-/-} mice. Scale bar: 100 μ m.

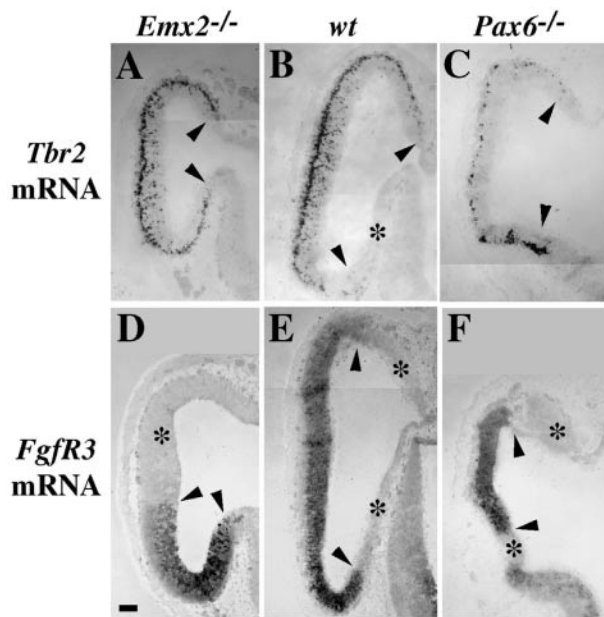


Figure 6. Distribution of *Tbr2* (A–C) and *Fgfr3* mRNA (D–F) on horizontal sections from cerebral cortex of *Emx2*^{-/-} (A, D), wild-type (B, E) and *Pax6*^{-/-} (C, F) E11 embryos; rostral is at the top. In wild-type embryos (B), *Tbr2* is expressed in numerous cells clustered in the marginal zone, as well as in scattered cells in the ventricular zone. The marginal subdomain extends from the rostral–medial pole up to the geometrical caudal pole of the vesicle (arrowheads); almost no positive cells can be detected in the caudal–medial sector (asterisk). Similar distribution of *Tbr2* transcripts can be detected in *Emx2*^{-/-} embryos (A); however, here numerous expressing cells can be found even in the caudal–medial sector, so that the caudal boundary of the marginal subdomain (arrowheads) is shifted at the tele-diencephalic junction. Only marginal *Tbr2* expressing cells can be found in *Pax6* null mutants (C), where they are distributed along the entire cortical perimeter; in this way, again, the caudal boundary of the expression domain (arrowheads) is shifted at the presumptive tele-diencephalic junction. In wild-type embryos (E), *Fgfr3* mRNA is expressed in a wide lateral domain (arrowheads) along a caudal-high to rostral-low gradient, and is undetectable in rostral–medial and caudal–medial sectors (asterisks). Similar distribution can be observed in *Pax6*^{-/-} mutants (F). In *Emx2*^{-/-} mutants (D), the caudal–medial negative domain is suppressed, the lateral positive domain is dramatically reduced in its axial extension and the rostral–medial negative domain remarkably enlarged. Scale bar: 100 μ m.

vesicle, or cortical hem (Roelink and Nusse, 1991; Grove *et al.*, 1998; Lee *et al.*, 2000). *Sfrp2*, encoding a putative secreted WNT antagonist, is specifically expressed near the cortico-striatal boundary, thus forming a lateral ‘mirror-image’ to the WNT-rich medial hem (Ragsdale *et al.*, 2000). Moreover, WNT signalling is crucial for growth of the cerebral cortex (Lee *et al.*, 2000; McLaughlin *et al.*, 2000; Galceran *et al.*, 2000). Therefore, scoring expression profiles of WNT signalling genes in wild-type, *Emx2* and *Pax6* null mutants should provide us with information about distributions of pre-areal values in the early cortical primordium of these mice; in addition, it could cast light onto molecular mechanisms controlling cortical growth. For these reasons, we systematically analysed *Wnt3a*, *Wnt8b* and *Sfrp2* expression domains in telencephalons of wild-type, *Emx2*^{-/-} and *Pax6*^{-/-} mice, at E11 (*Wnt3a* and *Wnt8b*) and E12.5 (*Sfrp2*).

In the cortical field of E11 wild-type embryos, *Wnt8b* mRNA is expressed along a medial–caudal high to rostral–lateral low gradient: its expression peaks in the cortical hem, is still detectable in the presumptive archicortex and fades out in the adjacent neocortical anlage (Fig. 4B). Complementary changes in the *Wnt8b* profile were found in *Emx2* and *Pax6* null brains (Fig. 4D,E). In *Emx2* knock-outs, the *Wnt8b* cortical domain was

restricted to a small area near the medial boundary of the cortical field (Fig. 4A); in *Pax6* null mutants, the *Wnt8b* domain was enlarged along the medial–lateral axis (Fig. 4C).

In wild-type embryos of the same developmental age, *Wnt3a* is restricted to the cortical hem (Fig. 4G,J,M, arrowheads); more specifically, its transcripts are detectable along the caudal 90% of the boundary between alar telencephalon and diencephalon (Fig. 4O,P). In *Emx2* null mice, *Wnt3a* was found to be severely down-regulated. Only a few cells expressing it could be detected in each frontal section, in the presumptive cortical hem (Fig. 4F,I,L, arrowheads); moreover, *Wnt3a* expression was restricted to only the caudal 60% of the telencephalic–diencephalic boundary (Fig. 4O,P). No major differences were found between *Wnt3a* expression profiles of *Pax6* null mutants and wild-type embryos (Fig. 4H,K,N, arrowheads; Fig. 4O,P); only some ectopic, scattered *Wnt3a*⁺ cells were detectable in the presumptive cortical field of *Pax6* mutants, more frequent in its medial–caudal part (Fig. 4H,K,N, arrows).

At E12, the presumptive WNT antagonist gene *Sfrp2* is normally expressed in the caudal ganglionic eminence (Fig. 5K, CGE) as well as in the lateral part of the lateral ganglionic eminence (l-LGE) or ventral pallium (Puelles *et al.*, 2000), in a long lateral, arc-shaped domain extending from the level of the CGE to cortical regions anterior to the foramen of Monro (Fig. 5E,H,K). This expression profile was dramatically impaired in both mutants under examination. In *Emx2* knock-outs, *Sfrp2* mRNA was confined to the CGE (Fig. 5J) and to the caudal-most l-LGE (Fig. 5G); no expression could be detected in intermediate and rostral l-LGE (Fig. 5A,D). Complete functional inactivation of *Sfrp2* was, conversely, found in the telencephalon of *Pax6* knock-outs (Fig. 5C,F,I,L).

Fgfr3 Expression Pattern in the Absence of Emx2 and Pax6

It has been reported that *Fgfr3* is expressed in a graded way in the early cortical primordium, with a caudal–lateral maximum and a rostral–medial minimum (Ragsdale *et al.*, 2000). We confirmed this report on E11 wild-type embryos. In particular, in horizontal sections taken from intermediate dorsal–ventral levels, we could distinguish a caudal–medial sector (Fig. 6E, asterisk), where no *Fgfr3* expression could be detected, a lateral sector displaying a caudal-high- to rostral-low-graded expression (Fig. 6E, delimited by arrowheads) and a rostral–medial sector, again free of any *Fgfr3* transcript (Fig. 6E, asterisk). Interestingly, in *Emx2*^{-/-} embryos, the rostral *Fgfr3*-free sector was substantially enlarged, the *Fgfr3*-positive caudal–lateral sector was reduced in its rostral–caudal extension, the caudal–medial *Fgfr3*-free domain was missing (Fig. 6D). No major changes in *Fgfr3* profile were found in *Pax6* null mutants (Fig. 6F).

Discussion

EMX2 and PAX6 Proteins are Both Necessary for Proper Expression of their mRNAs

It was already known that *Emx2* is normally expressed less intensely in regions of the cortical PVE where *Pax6* products are more abundant (Walther and Gruss, 1991; Gulisano *et al.*, 1996; Mallamaci *et al.*, 1998). Here, we have shown that, in the absence of either EMX2 or PAX6 proteins, expression of mRNA encoding the other one spreads to cortical regions where it is normally less abundant; this happens not only at E11, but even at later ages (data not shown). All this suggests that in the cortical PVE a direct mutual inhibition between *Emx2* and *Pax6* could normally occur.

In the absence of functional EMX2 protein, the expression of *Emx2* mRNA is down-regulated near the medial-caudal edge of its domain, where it is normally more intensely expressed. The fact that this down-regulation is not widespread, but can be detected just near this edge, provides clues about possible mechanisms by which *Emx2* normally sustains its own expression. It seems unlikely that self-sustainment takes place via a simple intracellular autoregulatory loop, which would occur everywhere in the cortical field. More reasonably, this phenomenon could rely on an intercellular positive feedback, specifically taking place near the caudal-medial boundary of the morphogenetic field in object and involving cells with special molecular and signalling properties (Meinhardt, 1983). These cells could be those forming the cortical hem, whose development is severely perturbed in *Emx2*^{-/-} mutants; WNT signalling, shown here to be deeply affected in these mutants, could be normally involved in this intercellular *Emx2* autoregulatory loop.

In the absence of functional PAX6 protein, the expression of *Pax6* mRNA is up-regulated near the medial-caudal edge of its expression domain, where it is normally less intensely expressed. In other words, down-regulation of *Pax6* by EMX2 requires PAX6, suggesting that these two proteins could provide this function as heterodimers. That would not be surprising: as recently reported, homeodomains of diverse proteins such as CHX10, SIX3, LHX2, EN1 and PREP1 bind to PAX6 and several can enhance *Pax6*-mediated transcriptional modulation upon co-expression in cells (Mikkola *et al.*, 2001).

Changes in the Cortical Molecular Protomap of *Emx2* and *Pax6* Null Mutants

Results of the molecular analysis reported above show that profound and coherent changes did occur in molecular regional profiles of both *Emx2*^{-/-} and *Pax6*^{-/-} cortical primordia at the onset of neuronogenesis.

In *Emx2*^{-/-} mutants, a pronounced enlargement of regions with rostral-lateral identity at the expense of those with caudal-medial identity was clearly detectable. In E11 *Emx2*^{-/-} brains, the relative transverse extension of the cortical *Emx1*⁺/*Tbr2*⁻ PVE, fated to give rise to archicortex and neocortex (Fernandez, 1998; Puelles *et al.*, 2000; Yun *et al.*, 2001), was reduced; remarkably, a reduction of the *Emx1*⁺ cortical domain was detectable in *Emx2*^{-/-} embryos even one day earlier, before the onset of cortical neuronogenesis. Moreover, the medial-most cortical PVE, expressing *Wnt8b* at higher levels and fated to give rise mainly to archicortex, was shrunken, especially near the caudal pole of the telencephalic vesicle. The rostral, *Wnt3a*⁻, cortical hem was enlarged at the expense of the caudal, *Wnt3a*⁺, hem. The rostral, *Fgfr3*⁻, cortical PVE was also enlarged, at the expense of the caudal-lateral, *Fgfr3*⁺, cortical PVE. Similarly, at E12.5, the rostral l-LGE domain, normally not expressing *Sfrp2*, was enlarged at the expense of the caudal l-LGE domain, normally expressing *Sfrp2*. Noticeably, the *Fgfr3*⁻ domain near the topological caudal edge of the vesicle was suppressed.

Complementary changes were found in the regionalization of the *Pax6* null cortical primordium. Expression of regional markers peculiar to the lateral-most cortical field was missing. The *Emx1*⁻/*Tbr2*⁺/*Mash1*⁻ l-LGE domain, presumptively fated to give rise to paleocortex, amygdala and claustrum (Fernandez, 1998; Puelles *et al.*, 2000; Stoykova *et al.*, 2000; Yun *et al.*, 2001), was not detectable at E11, in keeping with findings of Toresson *et al.* (Toresson *et al.*, 2000) and Yun *et al.* (Yun *et al.*, 2000); remarkably, the lateral *Emx1*⁻/*Mash1*⁻ domain was missing in the rostral forebrain even one day earlier, before

the onset of cortical neuronogenesis. At E12.5, the expression of *Sfrp2* mRNA within the l-LGE was also abolished (Kim *et al.*, 2001). Conversely, expression domains of medial cortical markers were wider. The *Wnt8b*⁺ cortical PVE, fated to give rise mainly to archicortex, was relatively enlarged; the *Wnt3a*⁺ domain, outlining the anlage of the hippocampal hem (Grove *et al.*, 1998), was also slightly enlarged, with ectopically localized *Wnt3a* positive cells within the dorsal neocortex.

It is noteworthy that the pattern alterations observed in the cortical primordium of *Emx2* and *Pax6* mutants at the beginning of neuronogenesis are coherent with distortions of areal profiles previously described in brains of the same mutants at late gestational ages, after the completion of neocortical neuronogenesis (Bishop *et al.*, 2000; Mallamaci *et al.*, 2000). It is also remarkable that these protomap misconfigurations were detected at the same developmental ages at which primary areal commitments were described to occur, or even before (Arimatsu *et al.*, 1992; Ferri and Levitt, 1993; Gitton *et al.*, 1999). This strongly suggests that late areal phenotypes of *Emx2* and *Pax6* mutants can be the consequence of an altered areal commitment of the cortical primordium in these mutants. Further experiments, including cortical transplantations from *Emx2*^{-/-} or *Pax6*^{-/-} donors to wild-type hosts and vice versa, will be necessary formally to prove this suggestion.

***Emx2*, *Pax6* and WNT Signalling**

The dramatic down-regulation of *Wnt3a* and *Wnt8b* expression taking place in *Emx2* null embryos is of particular interest. In these mutants, *Wnt3a* expression is almost abolished, being restricted to a few low-expressing cells near the caudal-medial pole of the telencephalic vesicle. This suggests a possible involvement of *Wnt3a* in the intercellular regulatory loop we hypothesized above to sustain *Emx2* expression near the caudal-medial pole of the cortical field. *Wnt8b*, still expressed in the cortical hem, is selectively down-regulated in presumptive archicortical and medial neocortical fields. This suggests the existence of two independent mechanisms governing *Wnt8b* expression in the alar forebrain: one active in the hem and not dependent on *Emx2*, the other one active in the cortex properly called and requiring the function of this gene. Remarkably, down-regulation of *Wnt* genes is associated with caudal confinement of the presumptive WNT antagonist *Sfrp2* (Rattner *et al.*, 1997), possibly as a consequence of the shift of intermediate portions of the *Emx2* null cortical primordium to more anterior regional identities. *Wnt3a* and *Wnt8b* expression alterations occurring in *Emx2* knock-out embryos are very similar to those described by Lee *et al.* (Lee *et al.*, 2000) in *Wnt3a* null mutants and provide valuable clues for a better understanding of early events leading to the abnormal late areal profile of the *Emx2* null cortex. It has been demonstrated that at E11, in the absence of *Wnt3a*, the proliferating fraction of cortical neuroblasts is normal in the lateral cortical anlage, but is significantly reduced near the cortical hem (Lee *et al.*, 2000). More recently, it has been reported that, after chronic administration of BrdU, the number of BrdU-labelled cells in the dentate gyrus is decreased by ~30% in adult *Wnt8b* knock-out mice as compared to wild-type controls (McLaughlin *et al.*, 2000). It is, therefore, reasonable to expect that knock-out of *Emx2* could result in reduced tangential growth of cortical medial-caudal regions. This suggests a dual origin for the late areal phenotype of these mutants, possibly arising from both distortion of the early cortical molecular protomap and reduced absolute growth of cortical regions committed to caudal-medial fates.

The detected up-regulation of *Wnt3a* and *Wnt8b* in *Pax6* null mice, i.e. the presence of scattered *Wnt3a* positive cells in the cortical field, near the hem, and the relative medial-lateral enlargement of the *Wnt8b* expression domain, suggests a crucial role for *Pax6* in confining WNT signalling to the caudal-medial cortical field. This suggestion is strengthened indeed by the absolute requirement of the *Pax6* function for the expression of the presumptive WNT antagonist *Sfrp2* in the lateral-most cortical field. It is tempting to speculate that up-regulation of *Wnt3a* and *Wnt8b* occurring in *Pax6* null embryos might have a functional consequence in promoting absolute tangential growth of caudal-medial regions in these mutants. In this way, as for *Emx2* null mutants, a dual origin can be hypothesized for the late areal phenotype of *Pax6* null mice, possibly arising from both distortion of the early cortical molecular protomap and reduced relative growth of cortical regions committed to rostral-lateral fates.

Notes

We wish to thank Alessandro Bulfone for the gift of the *Tbr2* cDNA clone and John Parnavelas for critical reading of the manuscript. This work was funded by the Italian Association for the Research against Cancer, Italian Telethon, Giovanni Armenise-Harvard Foundation, University Excellence Center on Physiopathology of Cell, CNR (Italian National Research Council) and EU (QLG3-CT-2000-00158, QLG3-CT-2000-01625, TMR HPRN-CT-2000-00097).

Address correspondence to Antonello Mallamaci, Molecular Biology of Development, DIBIT-HSR, via Olgettina 58, 20132 Milan, Italy. Email: mallamaci.antonio@hsr.it.

References

- Arimatsu Y, Miyamoto M, Nihonmatsu I, Hirata K, Uratani Y, Hatanaka Y, Takiguchi-Hayashi K (1992) Early regional specification for a molecular neuronal phenotype in the rat neocortex. *Proc Natl Acad Sci USA* 89:8879-8883.
- Barbe MF, Levitt P (1991) The early commitment of fetal neurons to the limbic cortex. *J Neurosci* 11:519-533.
- Barbe MF, Levitt P (1992) Attraction of specific thalamic input by cerebral grafts depends on the molecular identity of the implant. *Proc Natl Acad Sci USA* 89:3706-3710.
- Bishop KM, Goudreau G, O'Leary DD (2000) Regulation of area identity in mammalian neocortex by *Emx2* and *Pax6*. *Science* 288:344-349.
- Bovolenta P, Mallamaci A, Briata P, Corte G, Boncinelli E (1997) Implication of *Otx2* in pigmented epithelium determination and neural retina differentiation. *J Neurosci* 17:4243-4252.
- Briata P, Di Blas E, Gulisano M, Mallamaci A, Iannone R, Boncinelli E, Corte G (1996) EMX1 homeoprotein is expressed in cell nuclei of the developing cerebral cortex and in the axons of the olfactory sensory neurons. *Mech Dev* 57:169-180.
- Bulfone A, Martinez S, Marigo V, Campanella M, Basile A, Quaderi N, Gattuso C, Rubenstein JL, Ballabio A (1999) Expression pattern of the *Tbr2* (comesodermin) gene during mouse and chick brain development. *Mech Dev* 84:133-138.
- Donoghue MJ, Rakic P (1999) Molecular evidence for the early specification of presumptive functional domains in the embryonic primate cerebral cortex. *J Neurosci* 19:5967-5979.
- Fernandez AS, Pieau C, Reperant J, Boncinelli E, Wassef M (1998) Expression of the *Emx-1* and *Dlx-1* homeobox genes defines three molecularly distinct domains in the telencephalon of mouse, chick, turtle and frog embryos: implications for the evolution of telencephalic subdivisions in amniotes. *Development* 125:2099-2111.
- Ferri RT, Levitt P (1993) Cerebral cortical progenitors are fated to produce region-specific neuronal populations. *Cereb Cortex* 3:187-198.
- Galceran J, Miyashita-Lin EM, Devaney E, Rubenstein JL, Grosschedl R (2000) Hippocampus development and generation of dentate gyrus granule cells is regulated by LEF1. *Development* 127:469-482.
- Gitton Y, Cohen-Tannoudji M, Wassef M (1999) Specification of somatosensory area identity in cortical explants. *J Neurosci* 19:4889-4898.
- Grove EA, Tole S, Limon J, Ragsdale CW (1998) The hem of the embryonic cerebral cortex is defined by the expression of multiple *Wnt* genes and is compromised in *Gli3*-deficient mice. *Development* 125:2315-2325.
- Gulisano M, Broccoli V, Pardini C, Boncinelli E (1996) *Emx1* and *Emx2* show different patterns of expression during proliferation and differentiation of the developing cerebral cortex in the mouse. *Eur J Neurosci* 8:1037-1050.
- Hill RE, Favor J, Hogan BLM, Ton CCT, Saunders GF, Hanson IM, Prosser J, Jordan T, Hastie ND, van Heyningen V (1991) Mouse small eye results from mutations in a paired-like homeobox containing gene. *Nature* 354:522-525.
- Kim AS, Anderson SA, Rubenstein JLR, Lowenstein DH, Pleasure SJ (2001) *Pax-6* regulates expression of *SFRP-2* and *Wnt-7b* in the developing CNS. *J Neuroscience* 21:RC132.
- Kimura N, Nakashima K, Ueno M, Kiyama H, Taga T (1999) A novel mammalian T-box-containing gene, *Tbr2*, expressed in mouse developing brain. *Dev Brain Res* 115:183-193.
- Lee SMK, Shuba T, Grove E, McMahon A (2000) A local *Wnt-3a* signal is required for the development of the mammalian hippocampus. *Development* 127:457-467.
- McLaughlin DA, Price J, Mason J (2000) *Wnt8b* regulates cellular proliferation in the adult dentate gyrus. *Soc Neurosci* 2000:228.1.
- Mallamaci A, Iannone R, Briata P, Pintonello ML, Mercurio S, Boncinelli E, Corte G (1998) EMX2 in the developing mouse brain and in the olfactory area. *Mech Dev* 77:165-172.
- Mallamaci A, Muzio L, Chan CH, Parnavelas J, Boncinelli E (2000) Area identity shifts in the early cerebral cortex of *Emx2*^{-/-} mutant mice. *Nat Neurosci* 3:679-686.
- Mikkola I, Bruun JA, Holm T, Johansen T (2001) Superactivation of *Pax6*-mediated transactivation from paired domain-binding sites by DNA-independent recruitment of different homeodomain proteins. *J Biol Chem* 276:4109-4118.
- Meinhardt H (1983) Cell determination boundaries as organizing regions for secondary embryonic fields. *Dev Biol* 96:375-385.
- Miyashita-Lin EM, Hevner R, Montzka-Wassarman K, Martinez S, Rubenstein JLR (1999) Early neocortical regionalization in the absence of thalamic innervation. *Science* 285:906-909.
- Nakagawa Y, Johnson J, O'Leary DD (1999) Graded and areal expression patterns of regulatory genes and cadherins in embryonic neocortex independent of thalamocortical input. *J Neurosci* 19:10877-10885.
- O'Leary DDM (1989) Do cortical areas emerge from a protocortex? *Trends Neurosci* 12:400-406.
- Pellegrini M, Mansouri A, Simeone A, Boncinelli E, Gruss P (1996) Dentate gyrus formation requires *Emx2*. *Development* 122:3893-3898.
- Puelles L, Kuwana E, Puelles E, Bulfone A, Shimamura K, Keleher J, Smiga S, Rubenstein JL (2000) Pallial and subpallial derivatives in the embryonic chick and mouse telencephalon, traced by the expression of the genes *Dlx-2*, *Emx-1*, *Nkx-2.1*, *Pax-6*, and *Tbr-1*. *J Comp Neurol* 424:409-438.
- Ragsdale CW, Assimakopoulos S, Fukuchi-Shimogori T, Grove EA (2000) Early patterning of the cerebral cortex may be shaped by gradients of receptors and binding proteins of the *Fgf*, *Bmp* and *Wnt* signaling pathways. *Soc Neurosci* 2000:116.18.
- Rakic P (1988) Specification of cerebral cortical areas. *Science* 241:170-176.
- Rattner A, Hsieh JC, Smallwood PM, Gilbert DJ, Copeland NG, Jenkins NA, Nathans J (1997) A family of secreted proteins contains homology to the cysteine-rich ligand-binding domain of frizzled receptors. *Proc Natl Acad Sci USA* 94:2859-2863.
- Roberts RC (1967) Small eyes, a new dominant mutant in the mouse. *Genet Res* 9:121-122.
- Roelink H, Nusse R (1991) Expression of two members of the Wnt family during mouse development - restricted temporal and spatial patterns in the developing neural tube. *Genes Dev* 5:381-388.
- Simeone A, Gulisano M, Acampora D, Stornaiuolo A, Rambaldi M, Boncinelli E (1992) Two vertebrate genes related to *Drosophila empty spiracles* gene are expressed in embryonic cerebral cortex. *EMBO J* 11:2541-2550.
- Stoykova A, Gruss P (1994) Roles of *Pax* genes in developing and adult brain as suggested by expression patterns. *J Neurosci* 14:1395-1412.
- Stoykova A, Götz M, Gruss P, Price J (1997) *Pax6*-dependent regulation of adhesive patterning, R-cadherin expression and boundary formation in developing forebrain. *Development* 124:3465-3777.
- Stoykova A, Treichel D, Hallonet M, Gruss P (2000) *Pax6* modulates the

- dorsoventral patterning of the mammalian telencephalon. *J Neurosci* 20:8042-8050.
- Toresson H, Potter SS, Campbell K (2000) Genetic control of dorsal-ventral identity in the telencephalon: opposing roles for *Pax6* and *Gsh2*. *Development* 127:4361-4371.
- Walther C, Gruss P (1991) *Pax-6*, a murine paired box gene, is expressed in the developing CNS. *Development* 113:1435-1449.
- Yun K, Potter S, Rubenstein JLR (2000) *Gsh2* and *Pax6* play complementary roles in dorsoventral patterning of the mammalian telencephalon. *Development* 126:193-205.